

Article

Impact of Carbon Nanotubes and Graphene Oxide Nanomaterials on the Performance and Emissions of Diesel Engine Fueled with Diesel/Biodiesel Blend

Medhat Elkelawy , El Shenawy A. El Shenawy, Hagar Alm-Eldin Bastawissi  and Mahmoud M. Shams 

Mechanical Power Engineering Department, Faculty of Engineering, Tanta University, Tanta 31733, Egypt; hagaralmeldin@f-eng.tanta.edu.eg (H.A.-E.B.)

* Correspondence: medhatelkelawy@f-eng.tanta.edu.eg

Abstract: Biodiesel produced from waste cooked oil (WCO) resources mixed with various nanoparticle additives and used as a fuel blend in diesel engine combustion is a hopeful research trend. All previous studies indicate that alternative fuels can provide better fuel properties with enhanced engine combustion, performance, and lower emissions than fossil diesel fuel. This study uses three fuel blends to compare the diesel engine's combustion, performance, and emissions attributes at different loading values. Pure diesel fuel, B40, which is a blend of 40% WCO biodiesel and 60% diesel fuel, and mixtures of 40% WCO biodiesel, 56% diesel, and 4% toluene with carbon nanotubes (B40-CNTs) or graphene oxide nano-additive (B40-GO) at three concentrations of 50, 100, and 150 ppm were used. The results show enhancements in the diesel engine attribute values using B40-CNTs and B40-GO blends at different concentrations and engine load values better than the diesel engine attribute result values using B0 or B40 without nanoparticle additives. The combustion, performance, and emission attribute showed improvements using nanoparticles due to the increase in the evaporation rate, the oxygen rate, the surface area to volume ratio, and the thermal properties of the mixture. The highest in-cylinder peak pressure is recorded at 61 bar in B40 with 150 PPM of GO nanoparticles. The brake thermal efficiency records 43.6%, with the highest percentage found using B40-150GO at the maximum engine load value. The NO_x emissions are dropped from 1240 PPM using pure diesel fuel to 884 PPM using B40 with 150 PPM of GO nanoparticles at the maximum engine load due to the lower combustion temperatures and duration.

Keywords: diesel engine; waste cooking oil biodiesel; carbon nanotubes; graphene oxide nanoparticles



Citation: Elkelawy, M.; El Shenawy, E.S.A.; Bastawissi, H.A.-E.; Shams, M.M. Impact of Carbon Nanotubes and Graphene Oxide Nanomaterials on the Performance and Emissions of Diesel Engine Fueled with Diesel/Biodiesel Blend. *Processes* **2023**, *11*, 3204. <https://doi.org/10.3390/pr11113204>

Academic Editor: Miguel Ladero Galán

Received: 2 September 2023

Revised: 21 October 2023

Accepted: 31 October 2023

Published: 9 November 2023



Copyright: © 2023 by the authors. Licensee MDPI, Basel, Switzerland. This article is an open access article distributed under the terms and conditions of the Creative Commons Attribution (CC BY) license (<https://creativecommons.org/licenses/by/4.0/>).

1. Introduction

Nowadays, the massive consumption of fossil fuels in internal combustion engines can lead to fossil fuel depletion. The combustion of fossil fuels produces harmful exhaust gases that can change the climate and deteriorate the health of humans [1]. Diesel fuel can be wholly or partially substituted with biodiesel fuel from various resources in diesel engines, which is a green fuel with good combustion properties, including high burning ability and oxygenation [2,3].

Biodiesel can be produced cheaply using modernized technologies from various resources such as edible oil and nonedible and animal fat [4]. Note that direct oil from biodiesel resources cannot be applied to diesel engines as a fuel before converting to biodiesel fuels due to their high density, viscosity, and water content values [5]. The high viscosity can cause gum for the combustion chamber and injection components. The water content can cause corrosion and wear to the engine components [6].

Biodiesel from waste cooking oil can be produced using multiple manufacturing techniques such as pyrolysis, dilution, transesterification, and micro-emulsion [7]. Dilution can be achieved by mixing WCO at a maximum allowable percentage of 20% with fossil diesel fuel. Dilution for WCO can prevent engine damage causes [8]. Pyrolysis is an anaerobic

decomposition of the oil by heating without oxygen [9]. The micro-emulsion is a colloidal dispersion of fat combined with methanol or ethanol as a solvent to reduce viscosity and increase spraying quality [10]. Transesterification converts biodiesel resources to fatty acid methyl ester (FAME) and glycerol using alcohol like methanol and a catalyst [11]. There are four types of catalysts: acid, base, nano-catalyst, and enzyme [12]. Base catalysts have several benefits, such as availability, less energy requirement, fewer corrosion issues for engine components, and faster action than acid catalysts [13].

In a recent study [14], Cyclohexane was added by volume at 5, 10, and 15% as a flammable liquid to WCO biodiesel and diesel fuel in three blends: B60:D35C5, B60D30C10, and B60D25C15. The results showed that the engine performance and emission attributes improved if fuel blends were used compared to fossil diesel fuel. In addition, by increasing the injection pressure from 150 bars to 250 bars, the UHC, CO, and BSFC decreased. An experimental study was conducted using a single-cylinder diesel engine to compare the differences between two combustion modes, blend, add fuel combustion, and RCCI combustion. The blended fuel was biodiesel/n-butanol at various EGR rates, various timings of injection, and various loads of the engine. The optimum EGR percentage was 30%. The blended fuel mode maintained high BTE and low emissions but with high NO_x [15,16]. In addition, the advanced technology suggestions for improving the combustion and emissions characteristics were applied in conventional diesel engines [17,18]. The PPC engine concept was applied using an oxygenated and high-octane rating fuel such as methanol with different fuel injection strategies. In addition, the emissions reductions from using a low-carbon fuel such as alcohol reached 10% in some conditions compared with conventional engines.

Nanoparticles are the main elements in nanotechnology. Nanoparticles have a range of sizes from 1 nm to nearly 100 nm and have many shapes: cylindrical, spherical, and flat [19]. They can be crystalline or amorphous with zero, one, two, and three dimensions [20]. Nanoparticles can be classified according to their physical and chemical properties as organic, metal, ceramic, semiconductor polymeric, lipid, carbon-based, or composite nanoparticles [21]. The organic type is used mainly in medicine [22,23]. Metal nanoparticles and their oxides have good specifications for combustion in compression ignition engines due to their oxygen content, which can reduce harmful emissions and increase the surface area to volume ratio to increase the evaporation rate of the mixture [24–27].

Nanoparticles can be prevented from crumbling in the base fuel by using solvent and surfactant to increase the dissolving and guarantee the stability of the blend. Nanoparticles can be characterized and inspected through tests like X-ray diffraction (XRD), Brunauer–Emmett–Teller (BET), scanning electron microscopy (SEM), and transmittance electron microscope (TEM) tests. The nanoparticle production methods include the top-down and bottom-up production processes [28]. The top-down approach is a damaged technique for the most significant molecules that are transformed into small ones and converted to nanoparticles [29,30]. Moreover, a bottom-up process is a reverse approach for building up nanoparticles via spinning and atomic condensation.

The effect of using CeO₂ nanoparticles dispersed in biodiesel on the elemental carbon (EC), organic carbon (OC), size distribution, combustion, and emissions of the CRDI diesel engine is explored [31]. The diesel engine operated without a diesel particulate filter to prove that the emissions depend on the filter. The results indicated that adding CeO₂ nanoparticles to the biodiesel improved the in-cylinder pressure and the heat release rate. Using B15 with CeO₂ at 20 PPM, the Co and UHC significantly decreased, but NO_x emission increased compared to pure diesel. It was also observed that the B0 and B0C20 fuels produced particles with diameters more significant than the diameters of B10C20 and B15C20. The EC soot was higher than the OC for all fuels. The influence of CeO₂ nanoparticles on dual fuel and varied loads of diesel engines was studied. The CeO₂ nanoparticles were dispersed in methanol at 25 ppm and 100 ppm concentrations (MCN).

The diesel engine was operated in three modes: The first was direct injection mode. The second mode was injecting the methanol in the intake manifold, and the diesel fuel

was directly injected. The third mode injects the MCN in the intake manifold and injects the diesel fuel directly. It was observed that there was an increase in the peak in-cylinder pressure and the peak heat release rate using the MCN mode. The BTE and the BSFC were enhanced using the MCN compared to methanol mode. Most of the emissions were reduced using the MCN mode [32]. This paper [33] investigated the characteristics of the direct-injection diesel engine. Pure diesel fuel (D), WCO biodiesel (B), n-butanol (But), and titanium dioxide (TiO_2) nanoparticles were used. The test fuels were D100, B20, B20+ TiO_2 , B20But10, and B20But10+ TiO_2 . Adding TiO_2 increased the brake power and torque compared to using TiO_2 nanoparticles. Adding n-butanol and TiO_2 to the test fuels improved the peak in-cylinder pressure and the peak heat release rate compared to pure diesel. The CO, UHC, and smoke opacity emissions were reduced, and the NO_x emissions were reduced using n-butanol.

Carbon nanotubes (CNTs) are one of the significant nanoparticles. CNTs are described as nonmetal nanoparticles. CNTs have properties better than metal nanoparticles, such as high thermal conductivity [34]. CNTs can be used as a catalyst to nanofuels, improving the attributes of diesel engines by increasing the surface area to volume ratio, and thus the cetane number of the fuel [35]. The BTE of the diesel engine can be enhanced by adding CNTs due to the high chemical reactivity [36]. CNTs added to the diesel-water emulsion can produce better BTE than diesel-water only. Using CNTs in diesel engines can increase the peak in-cylinder pressure and shorten the combustion duration [37]. The peak heat release rate increases by dosing CNTs compared to base fuel only due to the high surface area to volume ratio, evaporation rate, and chemical reactivity [38].

CNTs have effective influences on the emissions produced by the diesel engine. CO emissions decreased with CNTs due to complete combustion, resulting from good blended fuel atomization and high surface area to volume ratio [39]. Also, the UHC emissions decreased due to combustion completion [40]. The reductions in NO_x emissions depend on the fuel type, the combustion duration, and the combustion temperatures. Low soot emissions are also observed using CNTs in diesel engines because of the high surface area to volume ratio and complete combustion.

Multiwalled carbon nanotubes (MWCNTs) were used with C. Inophyllum biodiesel and diesel blend (CIB20) to investigate the characteristics of diesel engines [41]. The MWCNTs were dispersed in the mix at 20, 40, 60, and 80 ppm concentrations. The results showed that the combination with MWCNTs at 60 ppm gave the highest percentage of BTE. All emissions were reduced with MWCNT compared to using CIB20 alone. Silicon dioxide (SiO_2) nanoparticles were used with methanol in diesel engine operation. The test fuels are diesel, diesel fuel with methanol, and finally, methanol diesel fuel with SiO_2 nanoparticles (MSN). The MSN fuel was injected into the intake manifold. It was observed that the peak in-cylinder pressure and heat release rate are increased in addition to enhancements in the BTE [42]. Nitrogen-doped multiwalled carbon nanotubes (N-doped MWCNTs) were used to enhance the attributes of the diesel engine. The MWCNTs were used as a reference for comparing with N-doped MWCNTs. The results showed enhancements in the engine attributes using N-doped MWCNTs [43].

Graphene oxide (GO) nanoparticles can be used in various applications, such as heat transfers. As nanoparticle additives, GO nanoparticles are used in diesel engine combustion due to their energy density, high thermal conductivity, and environmentally friendly [44,45]. GO nanoparticles can complete the combustion process due to the increased surface area to volume ratio, high chemical reactivity, and the existence of oxygen atoms [46]. GO nanoparticles were dispersed in biodiesel at B0, B10, and B20, and the GO concentrations were 30, 60, and 90 ppm, distributed via ultra-sonication [43]. The attributes of the diesel engine were investigated, and it was observed that GO nanoparticles enhanced the BTE and torque and reduced the BSFC. Also, reductions in CO and UHC emissions were observed, while increased CO_2 and NO_x emissions were reported.

Three nanoparticle additives GO, TiO_2 , and GO with TiO_2 , were used to study the characteristics of a cylinder diesel engine [47]. There was a reduction in BSFC of 12%

using diesel with TiO_2 fuel compared to pure diesel. The in-cylinder peak pressures using nanoparticle additive fuels were higher than those using pure diesel. Using TiO_2 and GO-TiO_2 with diesel fuel reduced the NO_x emissions formation and increased the CO emissions. In another study [48], GO nanoparticles at varying doses of 30, 60, and 90 PPM were added to the *Oenothera lamarchiana* biodiesel and diesel fuel (B20) blend to investigate the attributes of diesel engines. The results showed that the brake power, exhaust gas temperature, and CO_2 and NO_x emissions increased while the UHC and CO emissions were reduced. Single-walled carbon nanotubes, graphene oxide, and cerium oxide were used to investigate the characteristics of diesel engines at different loads [37]. A reduction in the combustion duration of 10.3%, the combustion advancing by 18.5%, an improvement in the BSFC of 15.2%, and a decrease in CO and UHC of 23.4% and 24.1%, respectively, were observed using single-walled CNTs at 25 PPM concentration.

In preparing the nanofuels, the dispersion of nanoparticles in the base fuel is one of the drawbacks. The method of nanoparticle distribution inside the original fuel is essential for enhancing the surface changes of nanoparticles due to the repulsion forces between all nanoparticles. Electrostatic dispersion is one method that can be attempted by coating the nanoparticles with a dispersing agent or surfactant [49,50]. The nanoparticle's surface is covered with the surfactant. Some changes are generated, producing repulsive forces between the nanoparticles in the base fuel. The surfactant amount must be maintained to act as the suitable coating, prevent repulsion, and compensate for the attraction forces of van der Waals. The type of surfactant can be classified into ionic surfactants and cationic surfactants [51,52].

The present study uses toluene (T) as a surfactant for dispersing GO or CNT nanoparticles in the fuel. Toluene was experimented with three percentages of the blend volume: 2%T, 4%T, and 6%T. It is observed that the ideal volume percentage is 4%T due to the stability and homogeneity of the blend and its ability to prevent the repulsion forces between the nanoparticles as much as possible.

The recent research aims to study the influence of nanoparticles dispersed in different blends of WCO biodiesel and diesel fuel on the combustion, performance, and emission attributes of single-cylinder, constant-speed diesel engines at varying loads. The nanoparticle types are CNTs or GO nanoparticles dispersed individually using toluene at 4% by volume in 56% fossil diesel fuel and 40% WCO biodiesel. The tested fuels are pure diesel (B0), a blend of WCO biodiesel at 40% and 60% diesel fuel (B40), and B40 with 50, 100, and 150 PPM of CNTs or GO nanoparticles.

2. The Procedure and the Experimental Setup

2.1. The Experimental Setup

A single-cylinder diesel engine test bench performs all the scheduled experiments. The tested engine is assembled with all the necessary equipment to measure the engine attributes. The test engine schematic diagram is presented in Figure 1. However, the whole system is pictured as shown in Figure 2. In addition, the tested engine specifications are displayed in Table 1. The engine is connected to an "ATE-160 LC" hydraulic dynamometer using a coupling to load the diesel engine and calculate the brake power at four specific loads. The hydraulic dynamometer's technical specifications are listed in Table 2. The diesel engine is supplied with Kistler 6125C01U20, an in-cylinder pressure transducer, to measure the in-cylinder pressure. The in-cylinder pressure transducer is connected to the charge amplifier and data acquisition system. The data acquisition is triggered with an optical crank angle encoder and is correlated with the top dead center (TDC) signal using a software application.

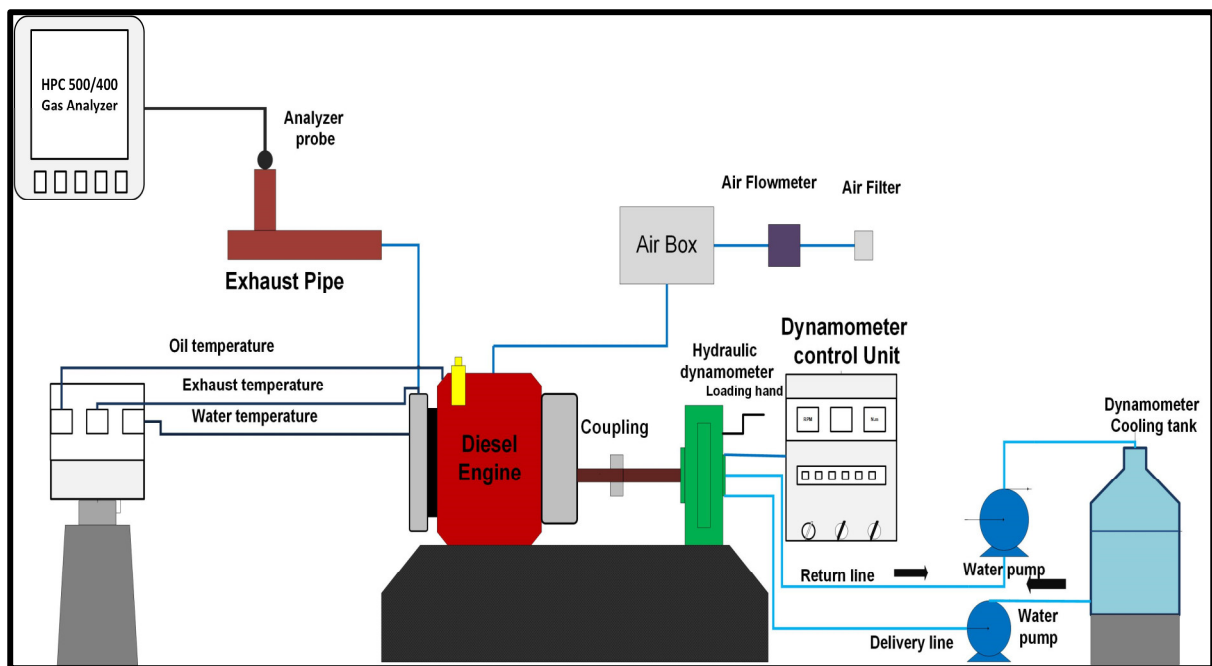


Figure 1. The test rig diagram.

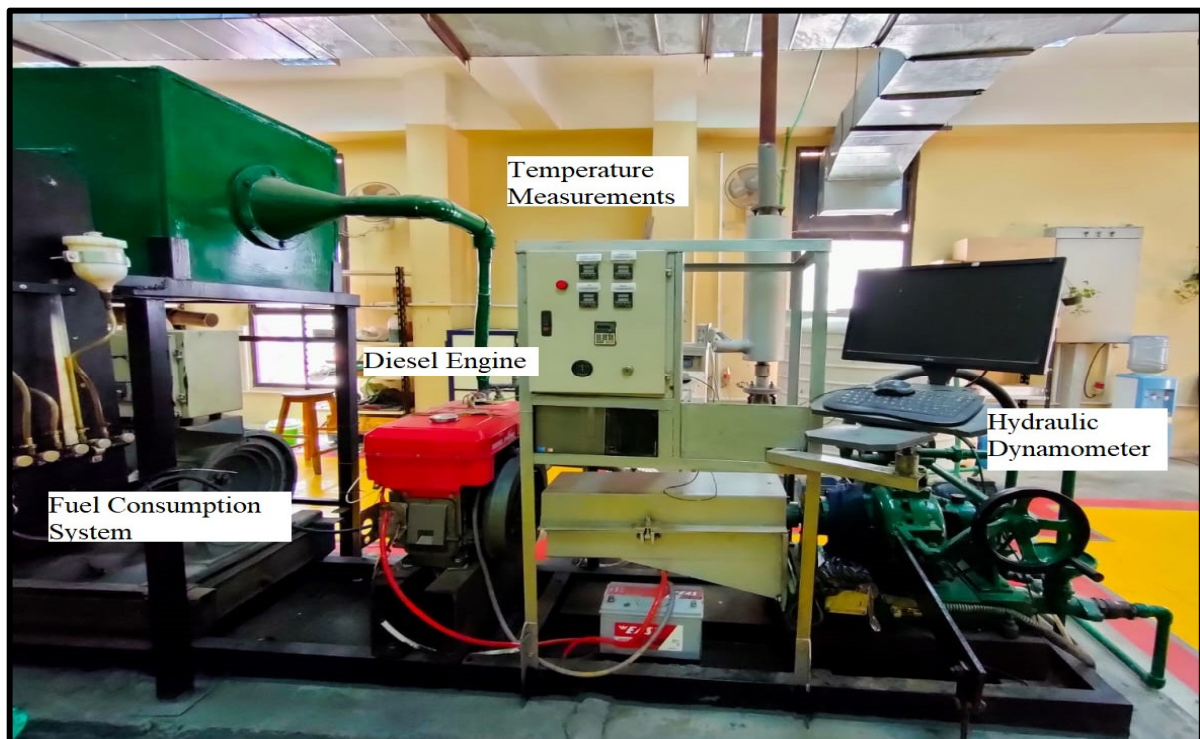


Figure 2. Photographic image of test bench equipment.

Table 1. The technical specifications of the ZS1115 diesel engine.

Parameter	Description
Model	ZS1115NM
Displacement	1.194
Bore × stroke	115 × 115 (mm)
Power rated	16.2/2200/min (kw/r/min)
Consumption of the fuel	≤242.1 (g/kW·h)
Cooling system	Condenser>
Starting method	Electric starting>
Lubrication system	Pressure/splash>
Net weight	185 (kg)
Compression ratio	17>

Table 2. “ATE-160 LC” hydraulic dynamometer technical data.

Dynamometer Trade Name	ATE-160 LC
Load cell capacity	(0–1050) (N·m)
Weight sensor	Load cell
Length of calibration lever arm	0.7645 m
Type of absorption	Water/Hydraulic
Dynamometer with engine connecting	Using half coupling

2.2. The Diesel Fuel and WCO Biodiesel Manufacturing

The specifications for the pure diesel fuel and WCO biodiesel are given in Table 3. The specifications of waste cooked oil biodiesel-diesel blend at 40% with 100 PPM of CNT or GO nano-additives are shown in Table 4. Waste cooked oil must be treated before being used as a biodiesel fuel. In this study, WCO is converted to biodiesel using a transesterification process. Transesterification is an approach to convert vegetable oil resources to fatty acid methyl ester (FAME) and glycerol. The transesterification approach has three steps, as shown in Figure 3: reaction, separation, and washing. The process was attempted by placing six liters of waste cooking oil with 1.2 L of methanol and 54 g of NaOH as a catalyst. Afterward, the mixing and heating of the ingredients are performed for an hour using a mixer rotating at a speed of 450 rpm and heated at 65 °C. In the separation process, the mixtures are left for one day to separate the biodiesel fuel from the glycerol. Finally, the washing process is attempted by feeding hot water at 100 °C with the biodiesel. After an hour, the WCO biodiesel will separate from the water and, by opening the bottom valve, the washing water gets out from the washing tank; the final product of WCO biodiesel fuel is then obtained.

2.3. The Carbon Nanotubes and Graphene Oxide Nanoparticles

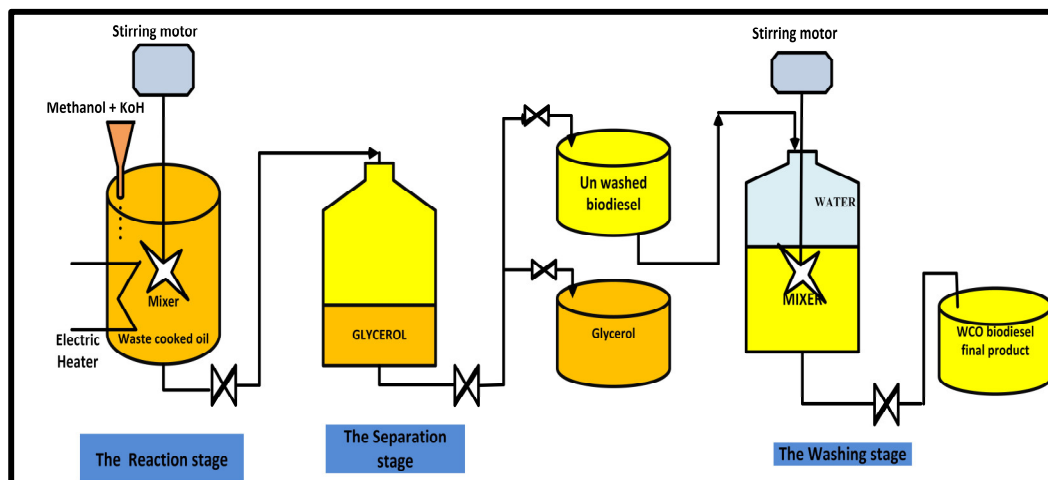
Two nanoparticle additives used in this study are CNTs and GO nanoparticles purchased from NanoTech Egypt CO, City of 6 October, Al Giza, Egypt. CNTs or GO nanoparticle additives used in the experiments are dispersed at 50, 100, and 150 PPM concentrations. The CNTs are inspected using transmittance electron microscope (TEM), as indicated in Figure 4, for size and structure inspection. Thermal gravimetric analysis (TGA) is used to inspect the thermal decomposition of the CNTs, as shown in Figure 5.

Table 3. Specifications of diesel and waste cooking oil biodiesel.

Specification	Diesel	WCO Biodiesel
Calorific value	42.10 MJ/kg	39.51 MJ/kg
Density	830 kg/m ³	875 kg/m ³
Cetane number	55	52
Flashpoint	45 °C	158 °C
Kinematic viscosity(cSt)@ 25 °C	3.14	5.13
Specific gravity	0.85	0.88
Auto ignition temperature	263 °C	273 °C
Cloud point	0 °C	6 °C
Oxygen content	0 (wt.%)	9.414 (wt.%)
Water content	0.05 (vol. %)	0.05 (vol. %)

Table 4. Specifications of diesel and waste cooking oil biodiesel with nano-additives.

Specification	B40 + 100 CNT	B40 + 100 GO
Calorific value	43.73 MJ/kg	44.4 MJ/kg
Density	846 kg/m ³	834 kg/m ³
Cetane number	55.8	56.1
Kinematic viscosity(cSt)@ 25 °C	5.07	5.02

**Figure 3.** Schematic diagram of WCO biodiesel production.

The GO nanoparticles are inspected using transmittance electron microscope (TEM) for size and structure inspection, as indicated in Figure 6. X-ray diffraction (XRD) is used to study the crystallographic structures. Surface-enhanced Raman spectroscopy (SERS) uses a Lab RAM HR 800 Laser Raman analyzer to inspect the surface properties. The properties of carbon nanotubes (CNTs) and graphene oxide (GO) nanoparticles are indicated in Table 5.

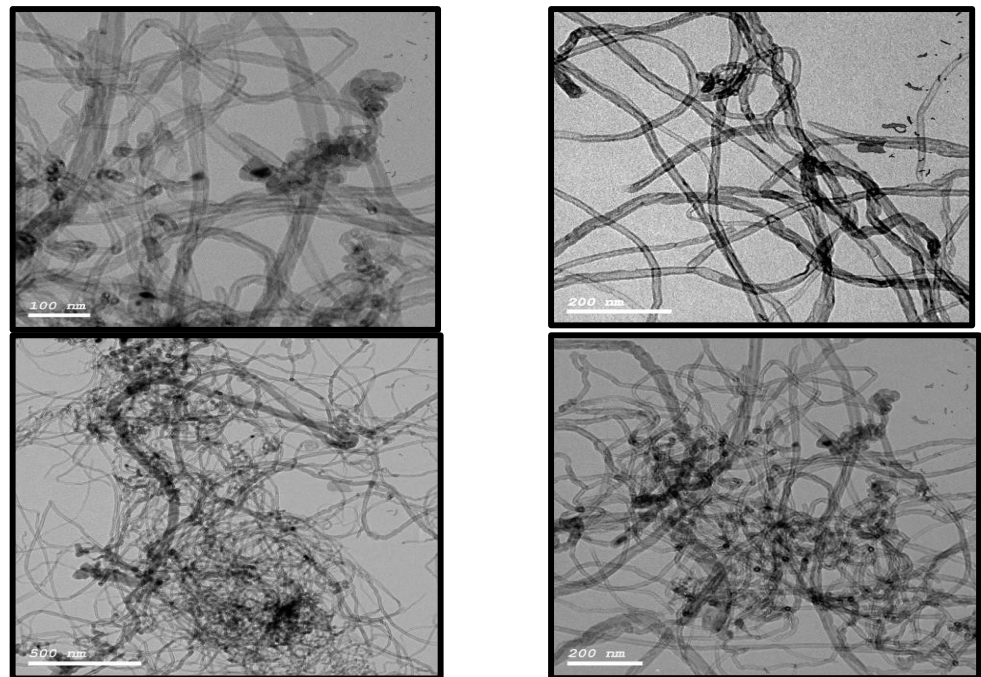


Figure 4. TEM micrograph for the CNTs.

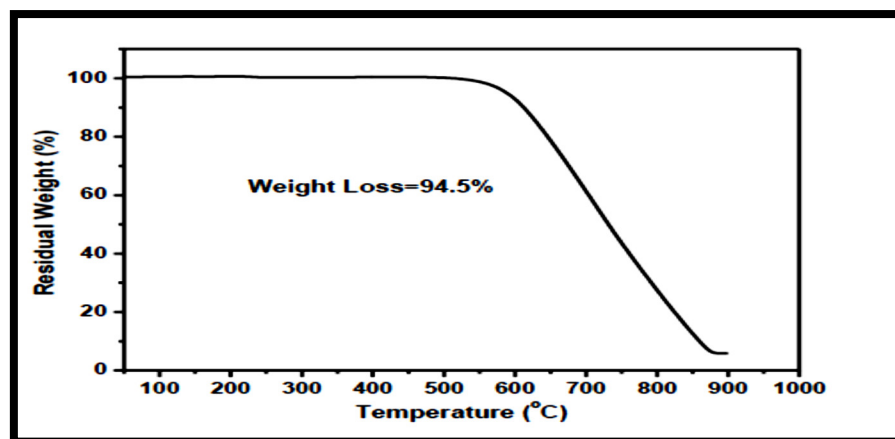


Figure 5. TGA thermo-gram of CNTs.

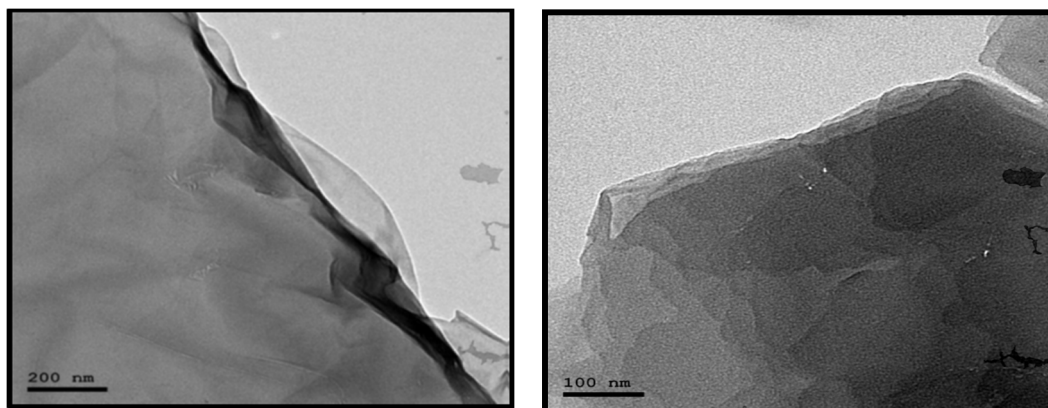


Figure 6. Transmittance electron microscopy for GO nanoparticles.

Table 5. Carbon nanotubes and graphene oxide specifications.

Specification	CNTs	GO
Color	Black	Brown black
Form	Powder	Powder
Ability of Solubility	Dispersed in water	Dispersed in water
Average Size	(L: >660 nm) and (D: 15 ± 7 nm)	Microns in length and a few nanometers in thickness
Purity	94.5%	-----
Shape (TEM)	Tubular-like shape	Sheets
Expiration Date	10/2023	11/2023

2.4. The Uncertainty Test

The produced temperatures in the experiments are measured using K-type thermocouples, and the data are viewed using a data logger. The thermocouples are placed to measure the cooling water temperatures, lubrication oil, and exhaust gases. Exhaust emissions such as oxygen (O₂), nitrogen oxides (NO_x), carbon monoxide (CO), carbon dioxide (CO₂), and un-burned hydrocarbon (UHC) emissions are measured using a Gas board 5020 analyzer. The smoke opacity is calculated using an AVL 415 S smoke meter. The errors are caused by factors like equipment error, measurements, the surroundings, and the measurement methods. All attributes are measured providing the diesel engine's stability and the uncertainties are calculated using the square root method and are listed in Table 6.

$$\text{The uncertainty} = \sqrt{(3)^2 + (0.5)^2 + (1)^2 + (1)^2 + (1)^2 + (0.4)^2} = \pm 3.522$$

Table 6. The uncertainty of the measuring equipment and performance.

Equipment	Uncertainty
Exhaust gas analyzer	$\pm 0.5\%$
Smoke meter	$\pm 3\%$
In-cylinder pressure transducer	$\pm 1\%$
In-cylinder pressure transmitter	± 1 Kpa
Temperature transmitter	± 1 deg.
Brake thermal efficiency	$\pm 0.4\%$

3. Results and Discussions

The present study investigates the effects of using pure diesel, a blend of WCO biodiesel with diesel fuel (B40), and combining CNTs or GO in B40 at various concentrations. The CNTs or GO concentrations are 50, 100, and 150 PPM. The experiments are carried out at different engine load values (0, 2, 4, 6, and 8 kW) at a constant engine speed of 1400 rpm. The diesel engine's combustion, performance, and emission attributes prove the benefits of using two different types of nanoparticles in addition to the waste cooked oil biodiesel in enhancing the characteristics of the diesel engine over and above the reduction in all emissions compared with the pure fossil diesel fuel.

3.1. Combustion Attributes

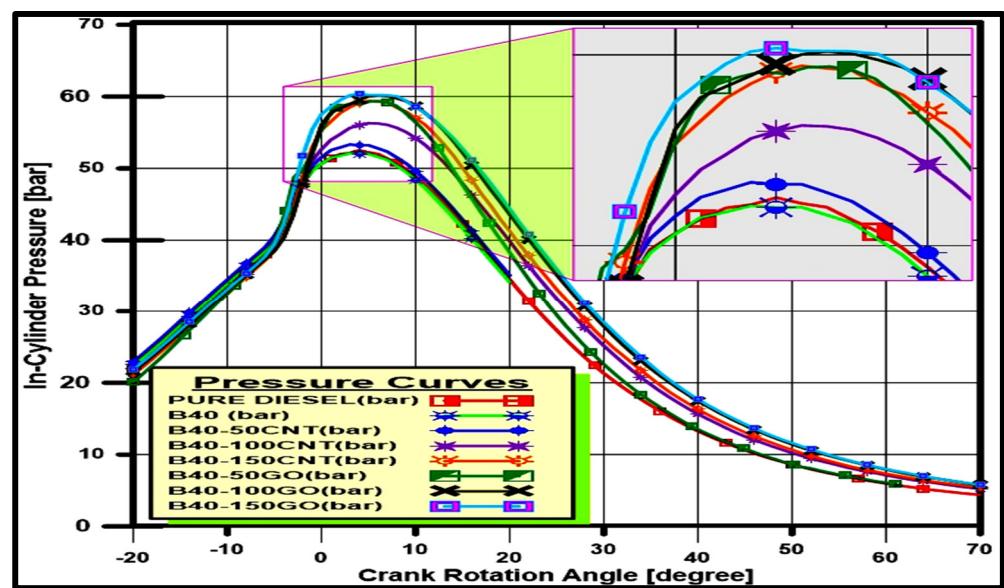
The influence of different nano-additives on pure diesel, B40, and B40 with various concentrations of GO nanoparticles or CNTs on diesel engine combustion is studied. Figure 7a illustrates the variations in the in-cylinder pressure for the tested fuels with varying crank angles at a constant diesel engine load of 4 kW. In contrast, Figure 7b shows the in-cylinder heat release rate at the tested conditions. From the graph, it is observed

that the peak in-cylinder pressures are recorded when using B40 with different concentrations of GO nanoparticles in comparison to the other fuels; the enhancement made in the combustion process was due to the high surface area to volume ratio and the high evaporation rate of the fuel droplets inside the combustion chamber which advances the ignition delay (ID) period and completes the combustion process in the controlled combustion phase. The highest in-cylinder peak pressure was recorded using B40 at 150 PPM of GO nanoparticles. Also, Figure 7b illustrates the relationship between the heat release rates (HRR) and varying the crank angle at constant load in the diesel engine. The graph shows HRRs are recorded using GO nanoparticles at different concentrations compared with the other fuels, and the highest value for the peak HRR occurred with B40 added by 150 PPM of GO nanoparticles. This phenomenon is observed due to GO nanoparticles that improve the premixed phase combustion, reducing the blended fuel's auto-ignition. However, the higher air-fuel utilization due to the micro explosion of the fuel droplets will dramatically increase the evaporation rate and shorten the combustion duration. However, because of the advancement of the reaction surface area and the increasing heat transfer rate of the fuel droplets by adding nanoparticles, it is easier to start the primary stage of combustion.

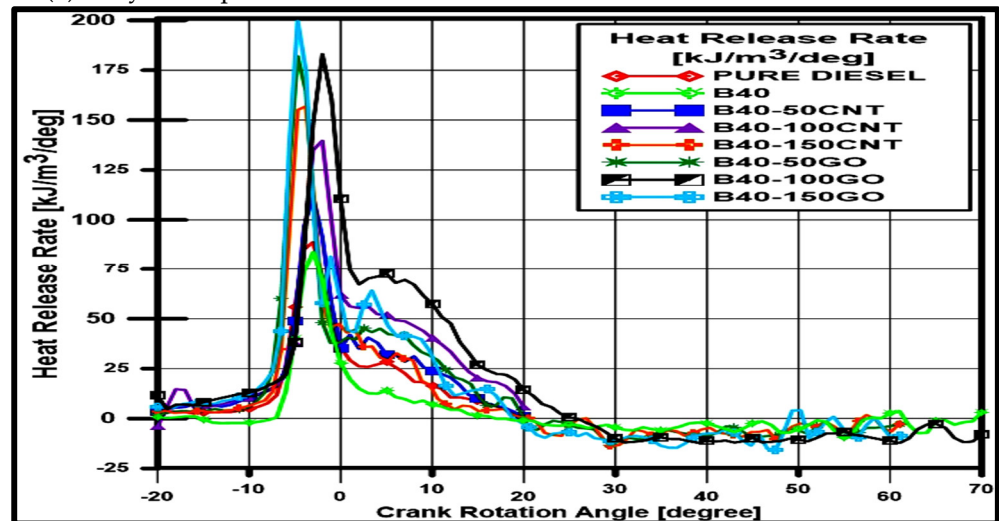
The combustion progression can be expressed by the combustion energy released, which is characterized by the location of the CA50. The combustion phasing can also be known by the crank angle position when 50% of the injected fuel was burned. The CA50 location is a significant factor through which we can predict the enhancement of the engine brake thermal efficiency and reduce all emissions. However, Figure 8 shows the location of CA50 at different engine loads for B0, B40, and B40 with various concentrations of CNTs or GO nanoparticles. From the graph, the areas of CA50 for fuels increase with an increase in the engine loads due to the rise in the amounts of the injected fuel mixture, although the turbulence in the mixture formation, the reduction in the ignition delay period, and the advances in the injection timing also have an impact. The locations of the CA50 in the case of using B40 with different concentrations of CNTs or GO nanoparticles were advanced compared to B40 or B0 at any specified engine loads. This is due to the enhancement in the fuel blend's thermal and physical properties using CNTs or GO nanoparticles. As mentioned, the high evaporation rate for the mixtures, the increase in the surface-to-volume ratio, the high oxygen content for the GO nanoparticles, and the predicted improvement for the spray characteristics will promote the combustion phasing or CA50 locations advancement when using CNTs or GO nanoparticles.

3.2. Performance Attributes

The influences of using pure diesel (B0), B40, and B40 at different concentrations of CNTs and GO nanoparticles on the engine performance were studied. Figure 9 shows the variation of BSFC for all the tested fuel blends at other engine loads and fixed speeds of 1400 RPM. It is noted that at the same engine load, by converting the fuel from B0 to B40, the BSFC increased due to increased WCO kinematic viscosity. This will reduce the spray characteristics inside the engine cylinder. By adding CNTs or GO nanoparticles to B40, the BSFC gradually decreased by increasing the concentrations due to the high evaporation rate of the fuel droplets and the increase in the surface area to volume ratio for B40-CNTs or B40-GO. With engine load increasing, the BSFC decreased, and the effect of using B40-GO can be compared with B40-CNT at varying concentrations due to oxygen atoms in the GO nanoparticles.



(a) In-cylinder pressure data at different nano-additives



(b) In-cylinder heat release rate data at different nano-additives

Figure 7. Effect of different nano additives on (a) in-cylinder pressure and (b) heat release rate relationships with crank rotation angle at 4 kW.

The BTE is the ability to convert the energy of combustion into mechanical work. Figure 10 indicates the influence of the fuel blends with different engine loads on the BTE. The BTE depends on the fuel properties like evaporation rate and chemical reactivity. It is observed from Figure 10 that at the same engine load, the BTE using B40 decreased compared to pure diesel. When CNTs or GO nanoparticles are added to B40 at different concentrations, the BTE percentages are increased compared to B0 and B40 due to the high evaporation rate, high oxygen content, advances in the ignition delay period and the increase in the surface area to volume ratio for B40-CNTs or B40-GO. By increasing the engine load, the BTE increased, and note that the effect of using B40-GO with different concentrations shows better results than that of B40-CNTs owing to the oxygen atoms in the GO nanoparticles.

The exhaust gas temperature (EGT) values are displayed in Figure 11. It is noted that by increasing the engine load values, the EGT values increase. EGTs for B0 have values higher than those of B40. Using nanoparticle fuels at different concentrations produces lower EGTs than B0 and B40 blends due to the decreased combustion duration and the advances in the ignition delay period. It is interesting to note that the B40-GO blends at

different concentrations give lower EGTs than B40-CNT. The previous research and results supported the present results [53].

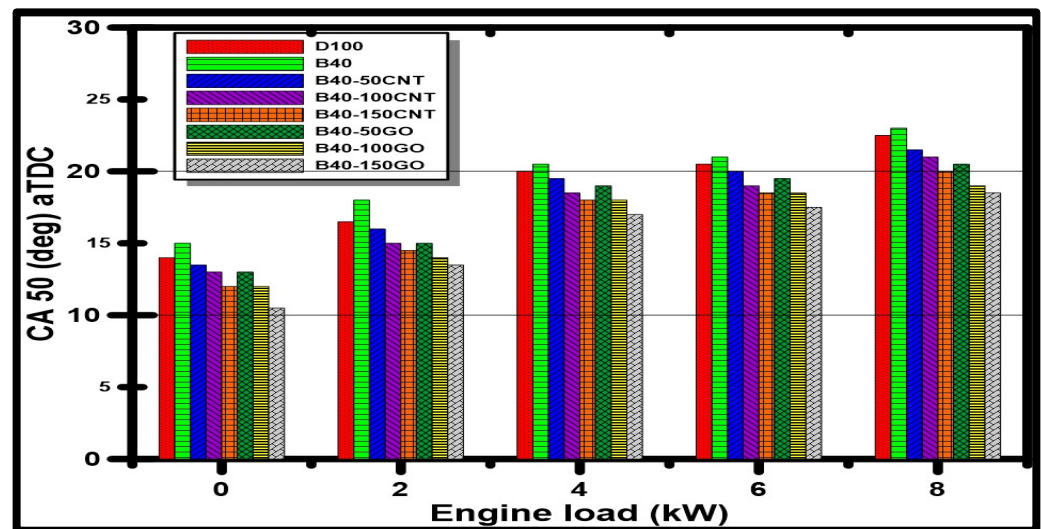


Figure 8. The relationship between the location of CA50 values and engine load.

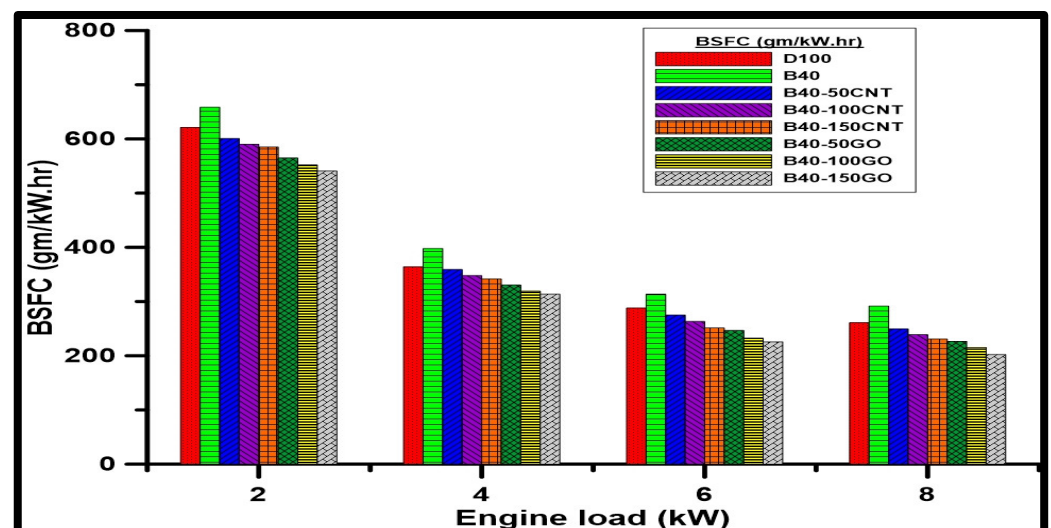


Figure 9. The relationship between BSFC values and engine load.

3.3. Emission Attributes

The influence of applying the fuel blends of B0, B40, B40-CNTs, and B40-GO on CO₂ emission is shown in Figure 12. The main variables influencing CO₂ emission are the temperature of combustion and the presence of oxygen atoms in the fuel blends. It is important to remember that the CO₂ level increases with completion of the combustion process inside the engine cylinder. As seen in Figure 12, the level of CO₂ increases with the increase in engine load due to the high combustion temperature and more combustion completion. The value of CO₂ using B40 is lower than that of B0 at the same engine load due to the reduction in evaporation rate for the fuel droplets inside the engine cylinder and the late ignition delay period of B40 compared to B0. Using B40-CNTs or B40-GO fuels at various concentrations will increase the combustion phasing and temperatures, increasing the CO₂ levels. Also, using B40-GO at different concentrations gives high CO₂ levels due to the existence of oxygen atoms and high evaporation rates in B40-GO, which increase the combustion temperatures.

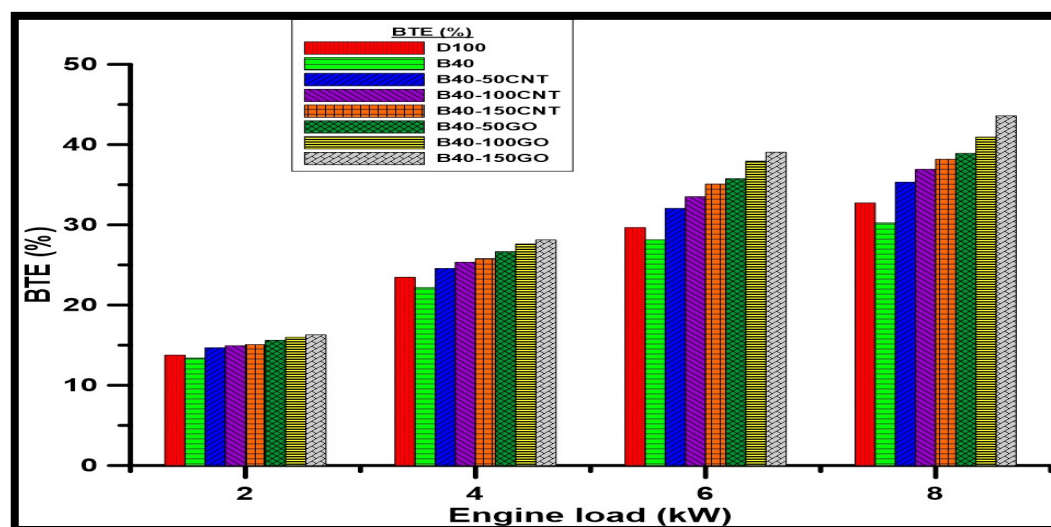


Figure 10. The relationship between BTE percentages and engine load.

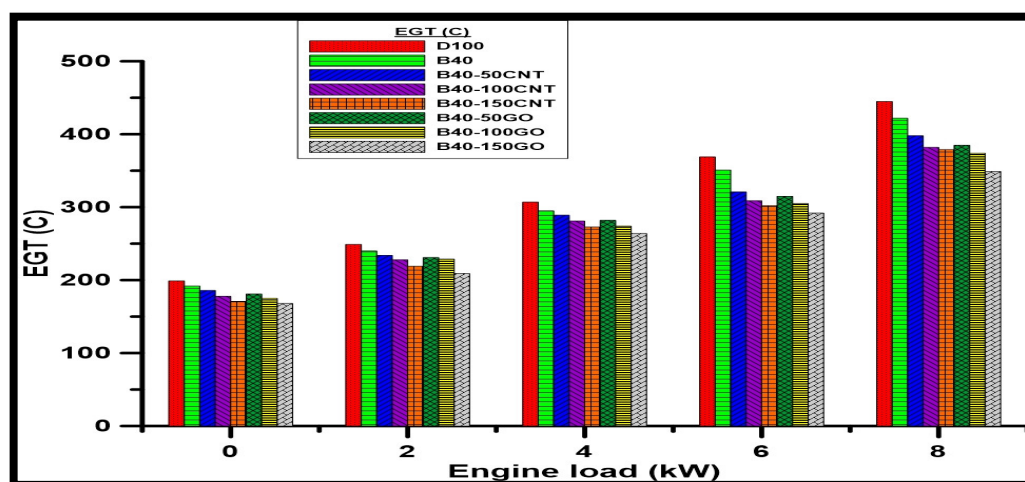


Figure 11. The relationship between EGT values and engine load.

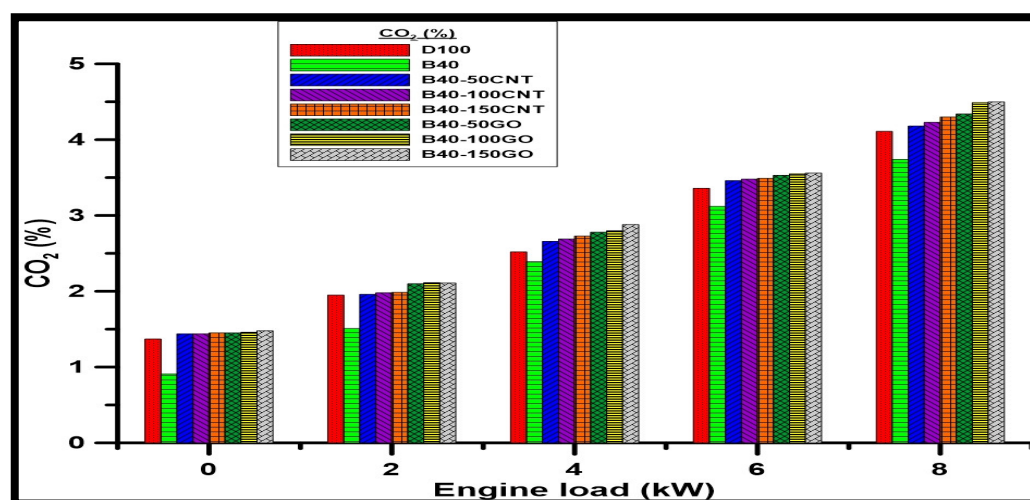


Figure 12. The relationship between CO₂ percentages and engine load.

NO_x emissions, which include NO, N₂O₂, and NO₂, have catastrophic effects on the environment and human beings. Several factors, such as fuel mixture properties, engine loads, combustion temperatures, and combustion duration, affect NO_x emissions.

Figure 13 shows that the NO_x emissions increase by increasing the engine load. However, with the use of B0, more NO_x emissions are produced compared with B40 due to the high combustion temperatures of B0. The NO_x emissions decrease once the nanoparticles are added due to the lowered combustion duration, which dramatically reduces the residence time of combustion, and the high thermal conductivity of the nanoparticles, representing as a heat sink and decreasing combustion temperatures [54].

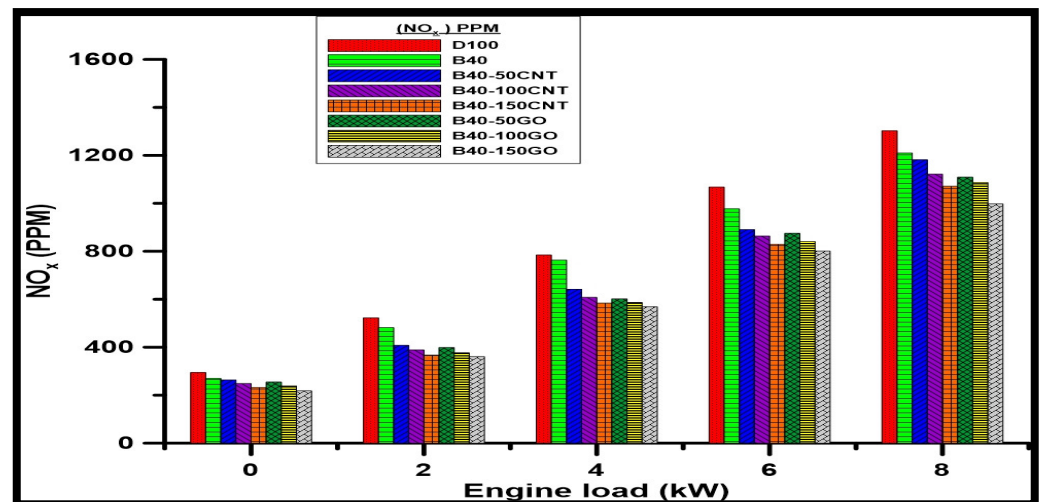


Figure 13. The relationship between NO_x emissions and engine load.

Unburned hydrocarbon (UHC) emissions are formed partly due to the lack of evaporation of the fuel and incomplete combustion. Figure 14 shows the influence of the fuel blends on UHC emissions at different engine loads at a fixed speed of 1400 RPM. It can be seen that UHC emissions increase with an increase in the engine load due to expanding the charge richness. By using B40 fuel, the UHC emissions were reduced again compared with B0 because of the existing oxygen content in WCO biodiesel, thus facilitating more complete combustion. Moreover, using nanoparticles decreases UHC emissions due to the high surface-to-volume ratio and enhancement made in the fuel droplets inside the engine. The UHC emissions decrease using B40-GO nanoparticles more than using B40-CNTs because of the increased oxygen content in the B40-GO nanoparticle blends [55].

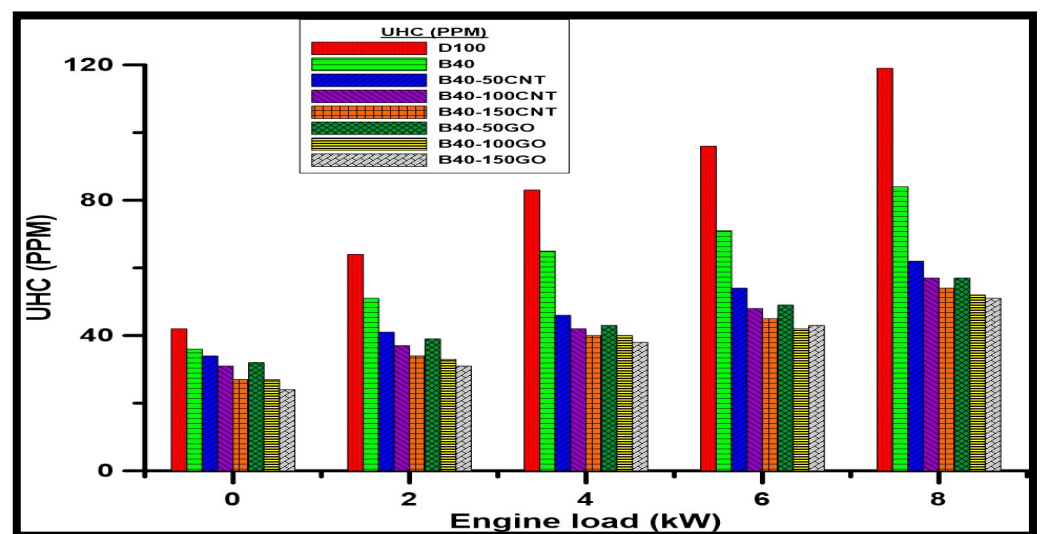


Figure 14. The relationship between UHC emissions and engine load.

The smoke opacity emission percentage decreases as a result of the complete combustion. Figure 15 shows the influence of the fuel quality on the smoke opacity emission percentage. It can be seen that the smoke opacity percentage increases with increasing the engine load. At the same load value, using B40 fuel, an oxygenated fuel, reduces the smoke opacity percentage emission compared with B0 because of the existing oxygen content in WCO biodiesel. Moreover, using nanoparticles decreases the smoke opacity percentage emission due to the high surface-to-volume ratio, which increases the chemical reactivity. The smoke opacity percentage emission decreases with the use of B40-GO nanoparticles compared with the help of B40-CNTs because of the high oxygen content in the B40-GO nanoparticle blends, and quicker completion of the combustion.

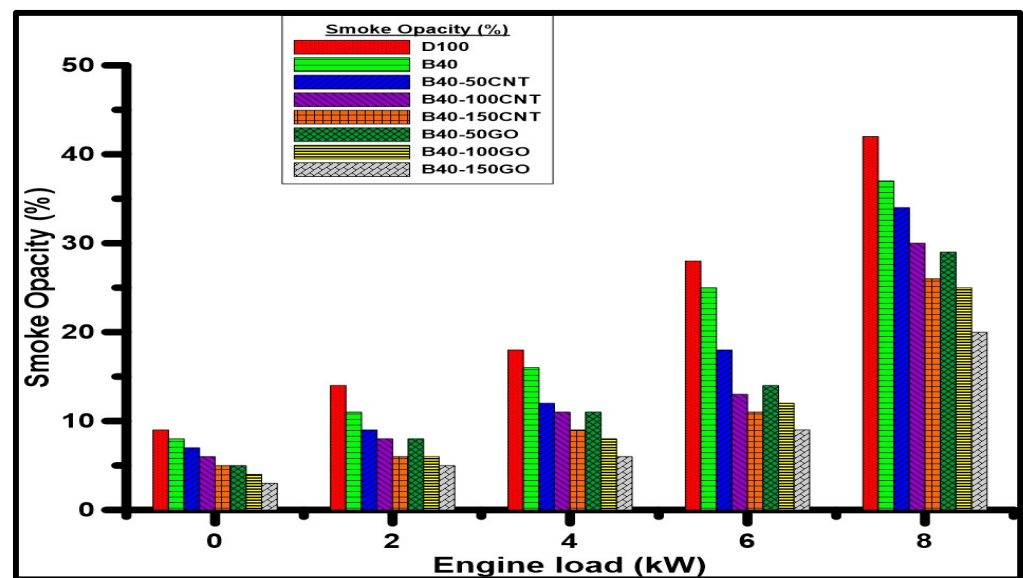


Figure 15. The relationship between smoke opacity emissions and engine load.

4. Cost Analysis

The cost of using CNTs or GO nanoparticles at various concentrations in diesel engine combustion to investigate the combustion, performance, and emission attributes can be analyzed as follows: The cost of one kg of B40 can cost 1.5 USD. The price of one gram of CNTs or GO nanoparticles is 33.5 USD. The concentrations of nanoparticles are 0.050 g, 0.100 g, or 0.150 g for one kg of 40% WCO biodiesel-diesel blend so can cost 3.175 USD, 4.85 USD, or 6.525 USD, respectively. The total cost for using B40 with 150 PPM of CNTs or GO nanoparticles at the maximum load (8 kW) according to the calculated BSFC is 1.5021 USD and 1.320 USD, respectively. The cost of using B40 only without nanoparticles at the total load (8 kW), according to the BSFC, is 0.437 USD. Therefore, the total cost of fuel is increased by adding nanoparticles because the nanoparticles are purchased commercially, which is so expensive. Still, the price will be lower if the nanoparticles are produced for mass production. Therefore, adding nanoparticles in diesel engine combustion has high utilities in conditions using low concentrations of nanoparticles in addition to lower produced emissions and lower BSFC. However, the total cost for B40 and 150 PPM of CNTs at 8 kW maximum engine load for one hour of the engine operation can be calculated as follow:

$$\begin{aligned}
 &\text{The total cost of B40 + 150PPM CNTs} = \\
 &(\text{total cost of one gm of B40 and 150PPM CNTs}) \times \text{BSFC} = \\
 &\left(\frac{6.525}{1000}\right) \times 230.22 = 1.5021 \text{ USD}
 \end{aligned}$$

Also, the total cost for B40 and 150 PPM of GO at 8 kW maximum engine load for one-hour operation is calculated as follows:

$$\begin{aligned} \text{The total cost of B40 + 150PPM GO} &= \\ (\text{total cost of one gm of B40 and 150PPM GO}) \times \text{BSFC} &= \\ \left(\frac{6.525}{1000}\right) \times 202.35 &= 1.320 \text{ USD} \end{aligned}$$

Finally, the total cost of B40 only at 8 kW maximum engine load is performed as follows:

$$\begin{aligned} \text{The total cost of B40} &= \\ (\text{total price of one gm of B40}) \times \text{BSFC} &= \\ \left(\frac{1.5}{1000}\right) \times 291.78 &= 0.437 \text{ USD} \end{aligned}$$

5. Conclusions and Future Work

A comprehensive study on the influence of using pure diesel (B0), B40, B40-CNTs, and B40-GO at three concentrations of 50, 100, and 150 ppm on the diesel engine attributes is investigated. From the results of the experiments, the conclusions are as follows:

1. The peak in-cylinder pressures are increased using different concentrations of nanoparticles due to the high surface area to volume ratio and the high evaporation rate.
2. The BSFC and BTE of B40-CNTs and B40-GO improved gradually with increasing nanoparticle concentrations and engine load compared to pure diesel (B0 and B40). Nanoparticle fuels also enhance exhaust gas temperatures (EGTs) due to the higher surface area to volume ratio oxygen content and the lowered combustion duration, which reduced the EGTs compared to B0 and B40.
3. The percentages of CO₂ levels increased with the increasing engine loads and with the use of nanoparticle fuels. B40-GO gives the highest CO₂ levels at different concentrations due to its high oxygen content, facilitating more complete combustion. Due to their high cetane number and oxygen content, NO_x emissions values are also low for the B40-CNTs and B40-GO nanoparticle fuels. Furthermore, the UHC emissions are significantly reduced using B40-CNTs and B40-GO nanoparticle fuels due to the increased surface area to volume ratio, increased evaporation, and more complete combustion.

The suggestions for future studies are to increase the concentrations of nanoparticles, use different types of nanoparticles, use different types of biodiesel, raise the percentage of biodiesel-diesel blends, use error bars in the Section 3, and use the response surface methodology (RSM) to examine numerous factors affecting the response variables of diesel engine combustion, performance, and emission attributes.

Author Contributions: H.A.-E.B., M.E., E.S.A.E.S. and M.M.S. suggested and planned the laboratory work. M.M.S. and M.E. carried out the experiments. All authors wrote, analyzed, discussed the results, and performed the final paper. All authors have read and agreed to the published version of the manuscript.

Funding: This research was funded by Tanta University Research Fund, grant code: tu: 02-19-01.

Data Availability Statement: All data used to support the findings of this study are included within the article.

Conflicts of Interest: The authors have no relevant financial or non-financial interests to disclose.

References

1. Kumaran, P.; Godwin, A.J.; Amirthaganesan, S. Effect of microwave synthesized hydroxyapatite nanorods using Hibiscus rosa-sinensis added waste cooking oil (WCO) methyl ester biodiesel blends on the performance characteristics and emission of a diesel engine. *Mater. Today Proc.* **2020**, *22*, 1047–1053. [[CrossRef](#)]
2. Marwaha, A.; Rosha, P.; Mohapatra, S.K.; Mahla, S.K.; Dhir, A. Waste materials as potential catalysts for biodiesel production: Current state and future scope. *Fuel Process. Technol.* **2018**, *181*, 175–186. [[CrossRef](#)]

3. Dimitrakopoulos, N.; Belgiorno, G.; Tuner, M.; Tunestal, P.; Di Blasio, G.; Beatrice, C. PPC Operation with Low RON Gasoline Fuel. A Study on Load Range on a Euro 6 Light Duty Diesel Engine. In Proceedings of the 9th International Symposium on Diagnostics and Modeling of Combustion in Internal Combustion Engines, Okayama, Japan, 25–28 July 2017; Volume 2017.9, p. C308.
4. Elkelawy, M.; Bastawissi, H.A.E.; El Shenawy, E.A.; Shams, M.M.; Panchal, H.; Sadasivuni, K.K.; Choudhary, A.K. Influence of lean premixed ratio of PCCI-DI engine fueled by diesel/biodiesel blends on combustion, performance, and emission attributes; a comparison study. *Energy Convers. Manag.* **2021**, *10*, 100066. [\[CrossRef\]](#)
5. Li, Z.; Zhang, Q.; Zhang, F.; Liang, H.; Zhang, Y. Investigation of Effect of Nozzle Numbers on Diesel Engine Performance Operated at Plateau Environment. *Sustainability* **2023**, *15*, 8561. [\[CrossRef\]](#)
6. De Araújo, C.D.M.; de Andrade, C.C.; e Silva, E.D.S.; Dupas, F.A. Biodiesel production from used cooking oil: A review. *Renew. Sustain. Energy Rev.* **2013**, *27*, 445–452. [\[CrossRef\]](#)
7. Singh, D.; Sharma, D.; Soni, S.L.; Inda, C.S.; Sharma, S.; Sharma, P.K.; Jhalani, A. A comprehensive review of biodiesel production from waste cooking oil and its use as fuel in compression ignition engines: 3rd generation cleaner feedstock. *J. Clean. Prod.* **2021**, *307*, 127299. [\[CrossRef\]](#)
8. Paone, E.; Tursi, A. 6—Production of biodiesel from biomass. In *Advances in Bioenergy and Microfluidic Applications*; Rahimpour, M.R., Kamali, R., Makarem, M.A., Manshadi, M.K.D., Eds.; Elsevier: Amsterdam, The Netherlands, 2021; pp. 165–192.
9. Jain, S.; Sharma, M.P. Prospects of biodiesel from *Jatropha* in India: A review. *Renew. Sustain. Energy Rev.* **2010**, *14*, 763–771. [\[CrossRef\]](#)
10. Koh, M.Y.; Ghazi, T.I.M. A review of biodiesel production from *Jatropha curcas* L. oil. *Renew. Sustain. Energy Rev.* **2011**, *15*, 2240–2251. [\[CrossRef\]](#)
11. Enweremadu, C.C.; Mbarawa, M.M. Technical aspects of production and analysis of biodiesel from used cooking oil—A review. *Renew. Sustain. Energy Rev.* **2009**, *13*, 2205–2224. [\[CrossRef\]](#)
12. Fonseca, J.M.; Teleken, J.G.; de Cinque Almeida, V.; da Silva, C. Biodiesel from waste frying oils: Methods of production and purification. *Energy Convers. Manag.* **2019**, *184*, 205–218. [\[CrossRef\]](#)
13. Khan, H.M.; Ali, C.H.; Iqbal, T.; Yasin, S.; Sulaiman, M.; Mahmood, H.; Raashid, M.; Pasha, M.; Mu, B. Current scenario and potential of biodiesel production from waste cooking oil in Pakistan: An overview. *Chin. J. Chem. Eng.* **2019**, *27*, 2238–2250. [\[CrossRef\]](#)
14. Elkelawy, M.; El Shenawy, E.A.; Khalaf Abd Almonem, S.; Nasef, M.H.; Panchal, H.; Bastawissi, H.A.E.; Sadasivuni, K.K.; Choudhary, A.K.; Sharma, D.; Khalid, M. Experimental study on combustion, performance, and emission behaviours of diesel /WCO biodiesel/Cyclohexane blends in DI-CI engine. *Process Saf. Environ. Prot.* **2021**, *149*, 684–697. [\[CrossRef\]](#)
15. Zheng, Z.; Xia, M.; Liu, H.; Shang, R.; Ma, G.; Yao, M. Experimental study on combustion and emissions of n-butanol/biodiesel under both blended fuel mode and dual fuel RCCI mode. *Fuel* **2018**, *226*, 240–251. [\[CrossRef\]](#)
16. Jin, C.; Zhang, X.; Geng, Z.; Pang, X.; Wang, X.; Ji, J.; Wang, G.; Liu, H. Effects of various co-solvents on the solubility between blends of soybean oil with either methanol or ethanol. *Fuel* **2019**, *244*, 461–471. [\[CrossRef\]](#)
17. Svensson, E.; Tuner, M.; Verhelst, S. Influence of injection strategies on engine efficiency for a methanol PPC engine. *SAE Int. J. Adv. Curr. Pract. Mobil.* **2019**, *2*, 653–671. [\[CrossRef\]](#)
18. Di Luca, G.; Picicelli, M.; Ianniello, R.; Belgiorno, G.; Di Blasio, G. Alcohol fuels in spark ignition engines. In *Application of Clean Fuels in Combustion Engines*; Springer: Berlin/Heidelberg, Germany, 2022; pp. 33–54.
19. Elias, A.; Saravanakumar, M. A review on the classification, characterisation, synthesis of nanoparticles and their application. *IOP Conf. Ser. Mater. Sci. Eng.* **2017**, *263*, 032019.
20. Machado, S.; Pacheco, J.G.; Nouws, H.P.A.; Albergaria, J.T.; Delerue-Matos, C. Characterization of green zero-valent iron nanoparticles produced with tree leaf extracts. *Sci. Total Environ.* **2015**, *533*, 76–81. [\[CrossRef\]](#)
21. Jeevanandam, J.; Barhoum, A.; Chan, Y.S.; Dufresne, A.; Danquah, M.K. Review on nanoparticles and nanostructured materials: History, sources, toxicity and regulations. *Beilstein J. Nanotechnol.* **2018**, *9*, 1050–1074. [\[CrossRef\]](#)
22. Allah, N.H.A.; Abouelmagd, S.A. Surface functionalization of polymeric nanoparticles for tumor drug delivery: Approaches and challenges. *Expert Opin. Drug Deliv.* **2017**, *14*, 201–214.
23. Elkelawy, M.; El Shenawy, E.A.; Bastawissi, H.A.E.; Shams, M.M.; Panchal, H. A comprehensive review on the effects of diesel/biofuel blends with nanofluid additives on compression ignition engine by response surface methodology. *Energy Convers. Manag.* **2022**, *14*, 100177. [\[CrossRef\]](#)
24. Tai, C.Y.; Tai, C.T.; Chang, M.H.; Liu, H.S. Synthesis of Magnesium Hydroxide and Oxide Nanoparticles Using a Spinning Disk Reactor. *Ind. Eng. Chem. Res.* **2007**, *46*, 5536–5541. [\[CrossRef\]](#)
25. Shamun, S.; Belgiorno, G.; Di Blasio, G.; Beatrice, C.; Tunér, M.; Tunestål, P. Performance and emissions of diesel-biodiesel-ethanol blends in a light duty compression ignition engine. *Appl. Therm. Eng.* **2018**, *145*, 444–452. [\[CrossRef\]](#)
26. Subramani, L.; Annamalai, K.; Parthasarathy, M.; Lalvani, I.J.R.; Moorthy, K. Production of *Garcinia gummi-gutta* methyl ester (GGME) as a potential alternative feedstock for existing unmodified DI diesel engine: Combustion, performance and emission characteristics. *J. Test. Eval.* **2018**, *46*, 20170246.

27. Yusuf, A.A.; Ampah, J.D.; Soudagar, M.E.M.; Veza, I.; Kingsley, U.; Afrane, S.; Jin, C.; Liu, H.; Elfasakhany, A.; Buyondo, K.A. Effects of hybrid nanoparticle additives in n-butanol/waste plastic oil/diesel blends on combustion, particulate and gaseous emissions from diesel engine evaluated with entropy-weighted PROMETHEE II and TOPSIS: Environmental and health risks of plastic waste. *Energy Convers. Manag.* **2022**, *264*, 115758.
28. Khan, I.; Saeed, K.; Khan, I. Nanoparticles: Properties, applications and toxicities. *Arab. J. Chem.* **2019**, *12*, 908–931. [\[CrossRef\]](#)
29. Behzad, F.; Naghib, S.M.; Tabatabaei, S.N.; Zare, Y.; Rhee, K.Y. An overview of the plant-mediated green synthesis of noble metal nanoparticles for antibacterial applications. *J. Ind. Eng. Chem.* **2021**, *94*, 92–104. [\[CrossRef\]](#)
30. Bello, S.A.; Agunsoye, J.O.; Hassan, S.B. Synthesis of coconut shell nanoparticles via a top down approach: Assessment of milling duration on the particle sizes and morphologies of coconut shell nanoparticles. *Mater. Lett.* **2015**, *159*, 514–519. [\[CrossRef\]](#)
31. Yusuf, A.A.; Inambao, F.L.; Ampah, J.D. The effect of biodiesel and CeO₂ nanoparticle blends on CRDI diesel engine: A special focus on combustion, particle number, PM_{2.5} species, organic compound and gaseous emissions. *J. King Saud Univ. Eng. Sci.* **2022**. [\[CrossRef\]](#)
32. Pan, S.; Wei, J.; Tao, C.; Lv, G.; Qian, Y.; Liu, Q.; Han, W. Discussion on the combustion, performance and emissions of a dual fuel diesel engine fuelled with methanol-based CeO₂ nanofluids. *Fuel* **2021**, *302*, 121096. [\[CrossRef\]](#)
33. Örs, I.; Sarıkoç, S.; Atabani, A.E.; Ünal, S.E.; Akansu, S.O. The effects on performance, combustion and emission characteristics of DIC engine fuelled with TiO₂ nanoparticles addition in diesel/biodiesel/n-butanol blends. *Fuel* **2018**, *234*, 177–188. [\[CrossRef\]](#)
34. Liu, M.S.; Lin, M.C.C.; Huang, I.T.; Wang, C.C. Enhancement of thermal conductivity with carbon nanotube for nanofluids. *Int. Commun. Heat Mass Transf.* **2005**, *32*, 1202–1210. [\[CrossRef\]](#)
35. Selvan, V.A.M.; Anand, R.B.; Udayakumar, M. Effect of Cerium Oxide Nanoparticles and Carbon Nanotubes as fuel-borne additives in Diesterol blends on the performance, combustion and emission characteristics of a variable compression ratio engine. *Fuel* **2014**, *130*, 160–167. [\[CrossRef\]](#)
36. Aalam, C.S.; Saravanan, C.G.; Kannan, M. Experimental Investigation on CRDI System Assisted Diesel Engine Fuelled by Diesel with Nanotubes. *Am. J. Eng. Appl. Sci.* **2015**, *8*, 380. [\[CrossRef\]](#)
37. Ooi, J.B.; Ismail, H.M.; Tan, B.T.; Wang, X. Effects of graphite oxide and single-walled carbon nanotubes as diesel additives on the performance, combustion, and emission characteristics of a light-duty diesel engine. *Energy* **2018**, *161*, 70–80. [\[CrossRef\]](#)
38. El-Seesy, A.I.; Abdel-Rahman, A.K.; Bady, M.; Ookawara, S.J. Performance, combustion, and emission characteristics of a diesel engine fueled by biodiesel-diesel mixtures with multiwalled carbon nanotubes additives. *Energy Convers. Manag.* **2017**, *135*, 373–393. [\[CrossRef\]](#)
39. Basha, J.S.; Anand, R.B. An experimental investigation in a diesel engine using carbon nanotubes blended water–diesel emulsion fuel. *Proc. Inst. Mech. Eng. A J. Power Energy* **2011**, *225*, 279–288. [\[CrossRef\]](#)
40. Basha, J.S.; Anand, R. Performance, emission and combustion characteristics of a diesel engine using Carbon Nanotubes blended Jatropa Methyl Ester Emulsions. *Alex. Eng. J.* **2014**, *53*, 259–273. [\[CrossRef\]](#)
41. Manigandan, S.; Sarweswaran, R.; Devi, P.B.; Sohret, Y.; Kondratiev, A.; Venkatesh, S.; Vimal, M.R.; Joshua, J.J. Comparative study of nanoadditives TiO₂, CNT, Al₂O₃, CuO and CeO₂ on reduction of diesel engine emission operating on hydrogen fuel blends. *Fuel* **2020**, *262*, 116336. [\[CrossRef\]](#)
42. Praveen, A.; Rani, G.J.; Balakrishna, B. Effect of MWCNTs as nano additives in C. Inophyllum biodiesel blend (CIB20) on the performance and emission parameters of a diesel engine. *Mater. Today Proc.* **2021**, *50*, 2581–2586. [\[CrossRef\]](#)
43. EL-Seesy, A.I.; Waly, M.S.; El-Batsh, H.M.; El-Zoheiry, R.M. Enhancement of the diesel fuel characteristics by using nitrogen-doped multiwalled carbon nanotube additives. *Process Saf. Environ. Prot.* **2023**, *171*, 561–577.
44. Hoseini, S.S.; Najafi, G.; Ghobadian, B.; Mamat, R.; Ebadi, M.T.; Yusaf, T. Novel environmentally friendly fuel: The effects of nanographene oxide additives on the performance and emission characteristics of diesel engines fuelled with Ailanthus altissima biodiesel. *Renew. Energy* **2018**, *125*, 283–294. [\[CrossRef\]](#)
45. Ooi, J.B.; Rajanren, J.R.; Ismail, H.M.; Swamy, V.; Wang, X. Improving combustion characteristics of diesel and biodiesel droplets by graphite oxide addition for diesel engine applications. *Int. J. Energy Res.* **2017**, *41*, 2258–2267. [\[CrossRef\]](#)
46. El-Seesy, A.I.; Hassan, H.; Ookawara, S. Effects of graphene nanoplatelet addition to jatropa Biodiesel–Diesel mixture on the performance and emission characteristics of a diesel engine. *Energy* **2018**, *147*, 1129–1152. [\[CrossRef\]](#)
47. Bello, Y.H.; Ookawara, S.A.; Ahmed, M.A.; El-Khouly, M.A.; Elmehasseb, I.M.; El-Shafai, N.M.; Elwardany, A.E. Investigating the engine performance, emissions and soot characteristics of CI engine fueled with diesel fuel loaded with graphene oxide-titanium dioxide nanocomposites. *Fuel* **2020**, *269*, 117436. [\[CrossRef\]](#)
48. Hoseini, S.S.; Najafi, G.; Ghobadian, B.; Ebadi, M.T.; Mamat, R.; Yusaf, T.J. Performance and emission characteristics of a CI engine using graphene oxide (GO) nano-particles additives in biodiesel-diesel blends. *Renew. Energy* **2020**, *145*, 458–465. [\[CrossRef\]](#)
49. El-Seesy, A.I.; Hassan, H. Investigation of the effect of adding graphene oxide, graphene nanoplatelet, and multiwalled carbon nanotube additives with n-butanol-Jatropa methyl ester on a diesel engine performance. *Renew. Energy* **2019**, *132*, 558–574. [\[CrossRef\]](#)
50. Vigneswaran, R.; Balasubramanian, D.; Sastha, B.D.S. Performance, emission and combustion characteristics of unmodified diesel engine with titanium dioxide (TiO₂) nano particle along with water-in-diesel emulsion fuel. *Fuel* **2021**, *285*, 119115. [\[CrossRef\]](#)
51. Paramashivaiah, B.M.; Banapurmath, N.R.; Rajashekhar, C.R.; Khandal, S.V. Studies on Effect of Graphene Nanoparticles Addition in Different Levels with Simarouba Biodiesel and Diesel Blends on Performance, Combustion and Emission Characteristics of CI Engine. *Arab. J. Sci. Eng.* **2018**, *43*, 4793–4801. [\[CrossRef\]](#)

52. Soudagar, M.E.M.; Nik-Ghazali, N.N.; Kalam, M.A.; Badruddin, I.A.; Banapurmath, N.R.; Ali, M.A.B.; Kamangar, S.; Cho, H.M.; Akram, N. An investigation on the influence of aluminium oxide nano-additive and honge oil methyl ester on engine performance, combustion and emission characteristics. *Renew. Energy* **2020**, *146*, 2291–2307. [[CrossRef](#)]
53. Nagaraja, S.; Rufuss, D.D.W.; Hossain, A.K. Microscopic characteristics of biodiesel—Graphene oxide nanoparticle blends and their Utilisation in a compression ignition engine. *Renew. Energy* **2020**, *160*, 830–841. [[CrossRef](#)]
54. Ramachander, J.; Gugulothu, S.; Sastry, G. Performance and Emission Reduction Characteristics of Metal Based SiO₂ Nanoparticle Additives Blended with Ternary Fuel (Diesel-MME-Pentanol) on CRDI Diesel Engine. *Silicon* **2021**, *14*, 2249–2263. [[CrossRef](#)]
55. Soudagar, M.E.M.; Nik-Ghazali, N.N.; Kalam, M.A.; Badruddin, I.A.; Banapurmath, N.; Khan, T.Y.; Bashir, M.N.; Akram, N.; Farade, R.; Afzal, A. The effects of graphene oxide nanoparticle additive stably dispersed in dairy scum oil biodiesel-diesel fuel blend on CI engine: Performance, emission and combustion characteristics. *Fuel* **2019**, *257*, 116015. [[CrossRef](#)]

Disclaimer/Publisher's Note: The statements, opinions and data contained in all publications are solely those of the individual author(s) and contributor(s) and not of MDPI and/or the editor(s). MDPI and/or the editor(s) disclaim responsibility for any injury to people or property resulting from any ideas, methods, instructions or products referred to in the content.